Evaluation of the OPLS-AA Force Field for the Study of Structural and Energetic Aspects of Molecular Organic Crystals

ARTICLE *in* THE JOURNAL OF PHYSICAL CHEMISTRY A · MARCH 2015

Impact Factor: 2.69 · DOI: 10.1021/jp512349r · Source: PubMed

2 AUTHORS, INCLUDING:

Carlos E S Bernardes
Centro de Química e Bioquímica, Faculdade d…

47 PUBLICATIONS **496** CITATIONS

THE JOURNAL OF PHYSICAL CHEMISTRY A

Article

pubs.acs.org/JPCA

Evaluation of the OPLS-AA Force Field for the Study of Structural and Energetic Aspects of Molecular Organic Crystals

Carlos E. S. Bernardes*[,†,‡] and Abhinav Joseph[‡]

[†]Centro de Química Estrutural, Instituto Superior Técnico, Universidade de Lisboa, Lisboa, Portugal

[‡]Centro de Química e Bioquímica e Departamento de Química e Bioquímica, Faculdade de Ciências, Universidade de Lisboa, Lisboa, Portugal

Supporting Information

ABSTRACT: Motivated by the need for reliable experimental data for the assessment of theoretical predictions, this work proposes a data set of enthalpies of sublimation determined for specific crystalline structures, for the validation of molecular force fields (FF). The selected data were used to explore the ability of the OPLS-AA parametrization to investigate the properties of solid materials in molecular dynamics simulations. Furthermore, several approaches to improve this parametrization were also considered. These modifications consisted in replacing the original FF atomic point charges (APC), by values calculated using quantum chemical methods, and by the implementation of a polarizable FF. The obtained results indicated that, in general, the best agreement between theoretical and experimental data is found when the OPLS-AA force field is used with the original APC or when these are replaced by ChelpG charges, computed at the MP2/aug-cc-pVDZ level of theory, for isolated molecules in the gaseous phase. If a good description of the energetic relations between the polymorphs of a compound is required then either the use of polarizable FF or the use of charges determined taking into account the vicinity of the molecules in the crystal (combining the ChelpG and MP2/cc-pVDZ methods) is recommended. Finally, it was concluded that density functional theory methods, like B3LYP or B3PW91, are not advisable for the evaluation of APC of organic compounds for molecular dynamic simulations. Instead, the MP2 method should be considered.

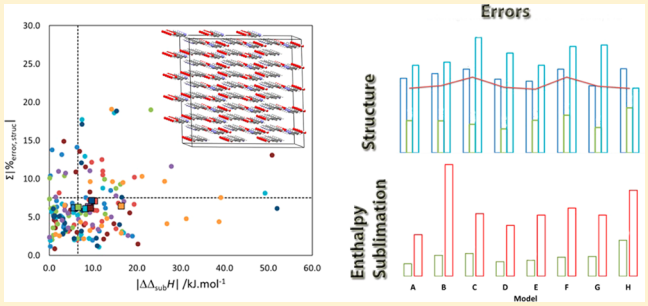

INTRODUCTION

Due to the increasing interest of the fine chemical industry, especially the pharmaceutical, in controlling and predicting the properties of solid organic materials, the application of theoretical methods to investigate different features of the solid state has become a hot topic.[1,2] From the different research areas in this field, prediction of the crystal structures of organic compounds and, thus, the possibility of occurrence of polymorphism, has attracted the attention of most of the theoretical scientific community.[1,3] In recent years, due to technical limitations of experimental methods to investigate, for example, solid−solid phase transitions and the formation of solids from solution (crystallization process), the use of theoretical methods has also gained importance as a reliable technique to obtain critical microscopic insight of these processes.[4]

The use of Molecular Dynamics (MD) simulations in conjunction with force fields that consider van der Waals and electrostatic interactions between the atoms, is one of the most promising and cost-effective computational approaches to study polymorphism and other aspects of the molecular solid state. The nonbonded interactions are, quite often, based on pre-established exp-6 Buckingham parametrizations (e.g., FIT and W99 potentials).[5−8] For the electrostatic interactions, due to the need of an accurate description of, for example, the hydrogen bonds that sustain the crystal structure, parameters determined for each system are generally used. These are normally obtained from the computation of ChelpG, RESP, and ESP atomic point charges (APC)[8−12] and by the use of the PIXEL[13] and distributed multipole electrostatic[14] models.

From the different methods to evaluate the electrostatic interactions, the use of the PIXEL and multipole electrostatic models are expected to give the more reliable interaction description between the molecules; however, currently they show some limitations:[13,14] (i) they are computationally more expensive than using APC; (ii) their use to study the dynamics of flexible molecules is difficult to implement; and (iii) for example, in the investigation of solids formation from solution, the compatibility of these approaches with well-established force fields for solvents, that normally use APC, is difficult to perform. Similarly, the nonbonded interactions described by exp-6 Buckingham functionals can also introduce some difficulties if (i) the simulations to be performed require the use of flexible molecules (the parametrization available for the

Received: December 11, 2014
Revised: February 20, 2015
Published: March 3, 2015

DOI: 10.1021/jp512349r
J. Phys. Chem. A 2015, 119, 3023−3034

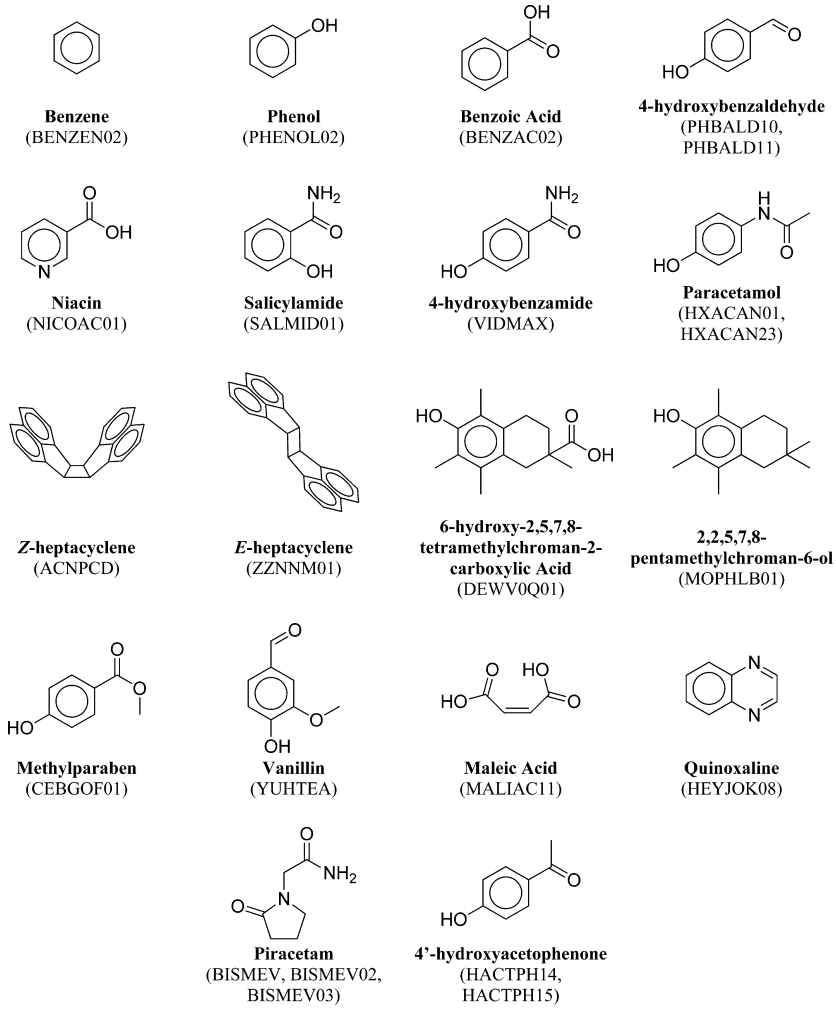

Figure 1. Compounds investigated in this work. The reference code in parentheses refers to the code in the Cambridge Structural Database for the crystal structure(s) of the compound.

description of the molecular flexibility with these force fields is limited)[5] and (ii) if the dynamics of formation of solids from solutions is to be investigated, relying on solvent parametrizations available in the literature, which normally use 12-6 Lennard-Jones potentials (e.g., AMBER, CHARMM, OPLS-AA).[15−19] For these reasons, quite often, an assessment of different force fields to describe the system under investigation is performed before the main investigation. Thus, the development/improvement of a force field fully compatible with those currently available in the literature, that can accurately describe the bonds, bending, torsions of organic molecules, and above all, could reproduce the experimental features of crystal structures, is desirable.

The validation of force fields normally requires the evaluation of its accuracy against reference experimental data, in this case, results of structural and energetic properties for a series of well-characterized materials.[9−11] For organic compounds, an ample structural databank is available, the Cambridge Structural Database,[20] which can be used to assess the performance of the methods to predict crystal structures. Very little information exists, however, for enthalpies of sublimation that can safely be assigned to a definite crystal structure and used as accurate benchmarks to validate lattice energy calculations.[9] Thus, this work is focused on two main goals: (i) the establishment of an experimental structural and energetic (enthalpies of sublimation) database that can serve as benchmarks for force fields evaluation and (ii) the use of the recommended data to investigate if molecular force fields currently available in the literature are suitable or can be improved to investigate solid materials. In this work, the well-established OPLS-AA force field,[18,19] that was specially developed to describe organic molecules in the liquid phase, was selected. This choice was based on the following criteria: (i) this parametrization has previously been proven to be able to reproduce structural and energetic features of solid materials[9] and (ii) it comprises a vast list of parameters to model bonds, angles, and dihedrals of organic molecules, allowing them to perform simulations with flexible molecules. In an attempt to improve the original OPLS-AA parametrization, several computational approaches to derive atomic point charges were tested. These included the use of APC computed by the ChelpG methodology[21] at different levels of theory, considering isolated molecules in the gaseous phase or small cluster of molecules mimicking the molecular arrangement in the crystal structure and also the use a polarizable model. These force field modifications were not accompanied by a reparametrization of the van der Waals parameters, although this type of interaction can have a large contribution to the computed properties.[22] This procedure, however, is not expected to significantly influence the computational results. In fact, as in the case of the OPLS-AA

DOI: 10.1021/jp512349r
J. Phys. Chem. A 2015, 119, 3023−3034

force field,[18] the transferability of the Lennard-Jones parametrization between similar atom types is normally a good approximation, when the atomic point charges of an atom are modified to account for a new local environment.

METHODS

The assessment of the performance of the OPLS-AA force field[18,19] and its modifications to reproduce the energetic and structural features of crystal structures was investigated from the study of 18 organic compounds and their known polymorphs. Figure 1 shows the molecules investigated in this work and the corresponding Cambridge Structural Database reference codes. The energetic data (i.e., enthalpies of sublimation) were taken from the literature or determined in this work.

General Information. X-ray powder diffraction analyses were carried out in the 2θ range 5−35° on a Philips PW1730 diffractometer, using a Cu Kα radiation source (θ = 1.5406 Å), with the tube amperage and voltage set to 30 mA and 40 kV, respectively. The samples were mounted in aluminum sample holders and the diffractogram collected with a 2θ step of 0.015° and a scan speed of 1.0 s/step, at ambient temperature (293 ± 2 K). The Celref program was used in the indexation of the powder pattern.[23]

An Agilent 6890 gas chromatograph coupled to an Agilent 5973N mass detector GC-MS was used to evaluate the sample purity. Helium was used as carrier gas and a capillary column TRB-5MS from Teknokroma selected for all experiments. Further details about the experimental conditions used in the sample purity evaluation can be found elsewhere.[24]

Materials. *Vanillin.* Vanillin (Sigma-Aldrich, 99%) was purified by sublimation at 300 K. A GC analyses revealed no impurities in the sample. The indexation of the powder X-ray diffractogram (see Table S1 of Supporting Information) indicated that the crystal structure of the purified material belongs to the monoclinic space group $P2_1$, with unit cell parameters a = 14.036 ± 0.026 Å, b = 7.876 ± 0.007 Å, c = 15.022 ± 0.028 Å, and β = 115.43 ± 0.14°, in good agreement with the reported structure by Velavan et al.:[25] space group $P2_1$, a = 14.049 ± 0.001 Å, b = 7.874 ± 0.008 Å, c = 15.017 ± 0.001 Å, and β = 115.45 ± 0.01°.

Maleic Acid. Maleic acid (Sigma-Aldrich, ≥99%) was used as received since, according to the supplier certificate (product 63180, lot BCBG8957 V), the amount of impurities in the sample was below the detection limit of a HPLC analysis. The indexation of the powder X-ray diffractogram (see Table S4 of the Supporting Information), indicated that the starting material crystal structure belongs to the monoclinic space group $P2_1/c$, with unit cell parameters a = 7.498 ± 0.032 Å, b = 10.129 ± 0.016 Å, c = 7.643 ± 0.033 Å, and β = 123.72 ± 0.28° and is in good agreement with the reported structure by James et al.:[26] space group $P2_1/c$, a = 7.473 ± 0.001 Å, b = 10.098 ± 0.002 Å, c = 7.627 ± 0.002 Å, and β = 123.59 ± 0.02°.

Methylparaben. Methylparaben (Sigma-Aldrich, ≥99%) was purified by sublimation at 336 K after recrystallization from DMSO. A GC analyses indicated a purity of 99.95% for the material. The indexation of the powder X-ray diffractogram (see Table S6 of Supporting Information) indicated that the crystal structure of the purified material belongs to the monoclinic space group Cc, with unit cell parameters a = 13.568 ± 0.036 Å, b = 16.943 ± 0.013 Å, c = 12.459 ± 0.032 Å, and β = 130.14 ± 0.14°, in good agreement with the reported structure by Xianti et al.:[27] space group Cc, a = 13.568 ± 0.005 Å, b = 16.959 ± 0.007 Å, c = 12.458 ± 0.006 Å, and β = 130.10 ± 0.03°.

Quinoxaline. Quinoxaline (Sigma-Aldrich, 99%) was used as received since, according to the supplier certificate (product Q1603, lot BCBG4535 V), the amount of impurities in the sample was below the detection limit of a GC analysis. The indexation of the powder X-ray diffractogram (see Table S8 of Supporting Information) indicated that the crystal structure of the purified material belongs to the orthorhombic space group $P2_12_12_1$, with unit cell parameters a = 4.018 ± 0.042 Å, b = 23.104 ± 0.038 Å, and c = 35.937 ± 0.057 Å, in good agreement with the reported structure by Sathishkumar et al.:[28] space group $P2_12_12_1$, a = 3.996 ± 0.002 Å, b = 23.022 ± 0.012 Å, and c = 35.822 ± 0.019 Å.

Enthalpy of Sublimation Determinations. The enthalpy of sublimation of vanillin (312.6 K), maleic acid (~376 K and ~394 K), quinoxaline (298.15 K), and methylparaben (338.0 K) were obtained by using the electrically calibrated twin-cell Calvet microcalorimeter previously described.[29,30] In general, the compound (2.2 to 21.9 mg) was placed inside a glass capillary and weighed with a precision of ±0.1 μg on a Mettler XP2U ultramicro balance. The capillary was dropped into the calorimeter cell under N_2 atmosphere. The signal corresponding to the heating of the sample from room temperature to the final temperature was then recorded and when it returned to the baseline, the sample and reference cells were simultaneously evacuated to 0.13 Pa. The measuring curve corresponding to the sublimation of the compound was finally acquired. The enthalpy of sublimation was found from the area of this curve, by using the energy equivalent of the apparatus determined by electrical calibration in a separate experiment. No residues of the samples were found inside the calorimetric cell at the end of the experiments.

As mentioned above, the enthalpies of sublimation of vanillin, maleic acid, and methylparaben, were measured above 298.15 K. Therefore, a correction of the results to this temperature was performed. This was achieved by using the heat capacities of the solid (taken from the literature or determined in this work by using a DSC 7 from PerkinElmer[31]) and gaseous phases. In the latter case, the heat capacities were computed with the Gaussian-03 program,[32] at the B3LYP/6-31G(d,p) level of theory,[33−35] using frequencies scaled by 0.961.[36] Further details about the enthalpy of sublimation corrections can be found in the Supporting Information.

Molecular Dynamics (MD) Simulations. All MD runs were performed using the DL-POLY classic.[37] The initial configurations of the simulation boxes were prepared using the program DLPGEN,[38] developed in the sequence of this work. This program produces approximate cubic simulation boxes, by stacking several unit cells taking into account their occupancy in the experimental crystalline structures. In all MD runs, a cutoff distance of 1.5 nm was selected and the Ewald summation technique applied to account for the electrostatic interactions beyond this limit. No corrections to the van der Waals contribution was performed, since the selected cutoff leads to marginal errors in the computed configurational energy (please see variation of the van der Waals energy as a function of the cutoff given in the Supporting Information). Details of the simulation boxes size, composition, and Ewald summation parameters are given as Supporting Information.

The simulations were performed at 298.15 K (with exception of benzene, that was simulated at 270 K) and 0.1 MPa, under the anisotropic isothermal−isobaric ensemble (N-σ-T), using a

DOI: 10.1021/jp512349r
J. Phys. Chem. A 2015, 119, 3023−3034

Nosé−Hoover thermostat and barostat, with relaxation time constants of 1 and 4 ps, respectively. Unless otherwise stated, all simulation boxes were equilibrated from the initial simulation box during 0.3 ns, before the production stage of 0.6 ns. Since the initial configurations were close to equilibrium, the relaxation was completed before the end of the equilibration period and extending the production run does not change significantly the obtained data. This is evident in the simulation results found for production stages with 0.6, 5, and 10 ns. As can be seen in the Supporting Information, differences well below the errors of the configurational energy (~0.5 kJ mol^{-1}) and structural parameters (typically 0.050 Å and 0.1° in the case of the cell lengths and angles, respectively) are found when the results obtained for a simulation with 0.6 ns are compared with one of 10 ns.

As mentioned above, the parametrization used in this work followed the OPLS-AA force field,[18,19] with the potential function defined in a general form as

$$U = \sum_{ij}^{\text{bonds}} \frac{k_{r,ij}}{2}(r_{ij} - r_{o,ij})^2 + \sum_{ijk}^{\text{angles}} \frac{k_{\theta,ijk}}{2}(\theta_{ijk} - \theta_{o,ijk})^2 + \sum_{ijkl}^{\text{dihedrals}} \sum_{n=1}^{3} \frac{V_{n,ijkl}}{2}[1 + (-1)^n \cos(n\varphi_{ijkl})] + \sum_i \sum_{j>i} \left\{ 4\varepsilon_{ij}\left[\left(\frac{\sigma_{ij}}{r_{ij}}\right)^{12} - \left(\frac{\sigma_{ij}}{r_{ij}}\right)^{6}\right] + \frac{q_i q_j}{4\pi\varepsilon_o r_{ij}} \right\} \quad (1)$$

where r_{ij} and $r_{o,ij}$ is the distance between atoms i and j and the corresponding equilibrium distance, respectively, θ_{ijk} and $\theta_{o,ijk}$ are the angle and equilibrium angle between atoms $i-j-k$, correspondingly, $k_{r,ij}$ and $k_{\theta,ijk}$ are the distance and angle force constants, respectively, $V_{n,ijkl}$ are Fourier coefficients for dihedral $i-j-k-l$ with angle φ_{ijkl}, σ_{ij} and ε_{ij} are the Lennard-Jones radii and well-depths, respectively, ε_o is the vacuum permittivity, and q_i and q_j are the atomic charges of atoms i and j, respectively. In eq 1, the three initial summations represent the decomposition of the potential energy into covalent bonds, valence angles, and torsion dihedral angles and were used to model the molecules as flexible. The last summation describes the van der Waals interactions, as Lennard-Jones (LJ) 12-6 potentials, and the Coulombic interactions, modeled as atomic point charges (APC). The electrostatic and LJ interaction between atoms in the same molecule separated by one or two bonds were ignored, while those separated by three were scaled by a factor of 0.5. Standard combination rules to determine the LJ parameters between different types of atoms were used, $\sigma_{ij} = (\sigma_i \cdot \sigma_j)^{1/2}$; $\varepsilon_{ij} = (\varepsilon_i \cdot \varepsilon_j)^{1/2}$, while the APC were obtained as described below. All input files used in the DL-POLY program were prepared with DLPGEN,[38] by using the list of parameters given as Supporting Information.

The standard molar enthalpy of sublimation, $\Delta_{sub}H^o_m$, of the compounds was estimated from

$$\Delta_{sub}H^o_m = U^o_{conf,m}(g) - U^o_{conf,m}(cr) + RT \quad (2)$$

where R = 8.3144621 J K^{-1} mol^{-1} is the gas constant,[39] T the temperature, $U^o_{conf,\,m}$ (cr) is the total molar configurational energy of solid phase and $U^o_{conf,\,m}$ (g) refers to the configurational energy of an isolated molecule in the gas phase. The term RT refers to the internal energy-to-enthalpy conversion assuming an ideal gas phase. The gaseous configurational energy was estimated via single-molecule simulations, under canonical $N-V-T$ ensemble conditions, using a Nosé−Hoover thermostat with relaxation time constants of 1 ps. Because of the poor statistics related with the small size of the simulation system, production runs of 40 ns were performed, and 20 such runs were considered to obtain an average $U^o_{conf,\,m}$ (g). In the case of compounds with more than one polymorph, the configurational energy in the gas phase was determined individually for each form. Indeed, quite often, the molecular configuration is different between polymorphs, thus leading to changes in $U^o_{conf,\,m}$ (g). If, however, the observed variation was within the calculation error, the average $U^o_{conf,\,m}$ (g) computed from the values obtained for the different phases was used in eq 2.

Electrostatic Models. As mentioned above, the description of electrostatic interactions is crucial in the simulation of solids. Therefore, in this work, several atomic point charges obtained by different models were considered, in the attempt to improve the ability of the original OPLS-AA force field parametrization to describe solid material: Model A refers to the use of the original APC given in the OPLS-AA force field parametrization.[22,23] Model B describes the transformation of model A into a polarizable force field, by adding a set of floating charges (Drude oscillators)[40,41] to the original model (see details below). In models C−F, the APC were evaluated for single molecules in the gaseous phase, using the ChelpG methodology[21] as implemented in the Gaussian 03 package.[32] Several theoretical methods were considered for the determination: MP2/cc-pVDZ,[42−46] MP2/aug-cc-pVDZ,[42−46] B3PW91/6-311+G(d,p),[33,47,48] and B3LPY/6-311+G(d,p)[33,34,48] for models C, D, E and F, respectively. In all cases, full geometry optimization of the molecular structure was performed prior to APC calculation at the same level of theory. In models G and H, the methodology previously described to obtain APC for the molecules within their electrostatic environment in the crystal structure was followed.[9,11] By this model, it is assumed that, for crystal structures where specific intermolecular interactions are present (e.g., hydrogen bonds), the APC of the molecules can be significantly altered relative to those computed for isolated molecules in the gaseous phase. Consequently, the computation of the APC is performed for a small aggregate mimicking the special relation between the molecules connected by hydrogen bonds (H bonds) in the crystal structure (please see examples in Supporting Information). The APC were then obtained by the ChelpG methodology at the MP2/cc-pVDZ[42−46] (model G) and B3PW91/6-311+G(d,p)[33,47,48] (model H) levels of theory, using the Gaussian 03 package,[32] without performing any structural optimization. The final APC for each molecule in the asymmetric unit were considered to correspond to those of the central molecule of the cluster. The fact that this procedure requires a small number of molecules to capture the electrostatic environment in the crystal structure allows the computation of the APC without the need for excessive computation resources and, more important, keeps the central molecule sufficiently exposed to avoid problems with buried atoms.[49] Finally, for crystal structures with more than one molecule in the asymmetric unit, the calculation of $U^o_{conf,\,m}$ (g) was performed using the average APC computed for each atom type.

From the analysis of Figure 1, it can be concluded that many of the compounds investigated in this work have atoms in equivalent positions and can exhibit fast and easy rotations (e.g., hydrogen atoms of methyl groups). For this reason, for all

DOI: 10.1021/jp512349r
J. Phys. Chem. A 2015, 119, 3023−3034

Table 1. Experimental Enthalpies of Sublimation, $\Delta_{sub}H^{o}_{m}$, and Corresponding Crystal Structure Details, Selected in This Work for the Establishment of a Benchmarks Database for Force Fields Assessment[a]

name	formula	CSD[b]	space group	Z'/Z	a/Å	b/Å	c/Å	α/deg	β/deg	γ/deg	$\Delta_{sub}H^{o}_{m}$/kJ mol^{-1}	refs
phenol	C_6H_6O	PHENOL02	$P2_122_1$	3/6	6.020	9.040	15.18	90.00	90.00	90.00	68.7 ± 0.5	55,56
4-hydroxybenzaldehyde - form I	$C_7H_6O_2$	PHBALD10	$P2_1/c$	1/4	6.453	13.810	7.044	90.00	107.94	90.00	99.7 ± 0.4	11,57
4-hydroxybenzaldehyde - form II	$C_7H_6O_2$	PHBALD11	$P2_1/c$	1/4	6.670	13.555	7.144	90.00	112.87	90.00	100.2 ± 0.4	11,58
benzoic Acid	$C_7H_6O_2$	BENZAC02	$P2_1/c$	1/4	5.500	5.128	21.950	90.00	97.37	90.00	89.7 ± 1.0	59,60
4′-hydroxyacetophenone - form I	$C_8H_8O_2$	HACTPH14	$P2_1/c$	1/4	7.720	8.360	11.280	90.00	95.02	90.00	103.2 ± 0.8	61
4′-hydroxyacetophenone - form II	$C_8H_8O_2$	HACTPH15	$P2_12_12_1$	2/8	6.110	9.529	24.313	90.00	90.00	90.00	104.3 ± 0.4	61
nicotinic acid	$C_7H_6NO_2$	NICOAC01	$P2_1/c$	1/4	7.162	11.703	7.242	90.00	113.20	90.00	112.1 ± 0.5	62,63
salicylamide	$C_7H_7NO_2$	SALMID01	$I2/a$	1/8	12.901	4.982	20.987	90.00	91.50	90.00	101.9 ± 0.4	24,64
4-hydroxybenzamide	$C_7H_7NO_2$	VIDMAX	$P2_1/c$	1/4	4.583	8.825	15.888	90.00	90.77	90.00	129.7 ± 1.6	24,65
benzene[c]	C_6H_6	BENZEN02	$Pbca$	1/4	7.46	9.66	7.03	90.00	90.00	90.00	45.0 ± 0.1	66−68
Z-heptacyclene	$C_{24}H_{16}$	ACNPCD	$P2_1/c$	1/4	11.966	13.930	10.003	90.00	107.70	90.00	128.5 ± 2.3	69,70
E-heptacyclene	$C_{24}H_{16}$	ZZNNM01	$P2_1/n$	1/2	7.827	4.865	20.221	90.00	92.79	90.00	149.0 ± 3.1	70
paracetamol - form I	$C_8H_9NO_2$	HXACAN01	$P2_1/a$	1/4	12.930	9.400	7.100	90.00	115.90	90.00	129.7 ± 1.6	71,72
paracetamol - form II	$C_8H_9NO_2$	HXACAN23	$Pcab$	1/8	7.406	11.837	17.162	90.00	90.00	90.00	127.7 ± 1.6	72,73
piracetam - form I	$C_6H_{10}N_2O_2$	BISMEV03	$P2_1/n$	1/4	6.747	13.418	8.090	90.00	99.01	90.00	119.3 ± 1.4	74,75
piracetam - form II	$C_6H_{10}N_2O_2$	BISMEV	$P\bar{1}$	1/2	6.403	6.618	8.556	79.85	102.39	91.09	122.5 ± 1.4	75,76
piracetam - form III	$C_6H_{10}N_2O_2$	BISMEV02	$P2_1/n$	1/4	16.403	6.417	6.504	90.00	92.05	90.00	122.8 ± 1.4	75,77
methylparaben[d]	$C_8H_8O_3$	CEBGOF	Cc	3/12	13.568	16.959	12.458	90.00	130.10	90.00	106.2 ± 0.9	27
2,2,5,7,8-pentamethylchroman-6-ol	$C_{14}H_{20}O_2$	MOPHLB01	$P\bar{1}$	2/4	10.843	13.304	9.155	103.68	97.18	91.05	107.4 ± 0.8	78,79
6-hydroxy-2,5,7,8-tetramethylchroman-2-carboxylic acid	$C_{14}H_{18}O_4$	DEWV0Q01	$P2_1/c$	1/4	10.829	11.106	11.152	90.00	109.32	90.00	136.9 ± 2.5	79,80
vanillin[d]	$C_8H_8O_3$	YUHTEA	$P2_1$	4/8	14.049	7.874	15.017	90.00	115.45	90.00	95.0 ± 0.5	25
maleic acid[d]	$C_4H_4O_4$	MALIAC11	$P2_1/c$	1/4	7.473	10.098	7.627	90.00	123.59	90.00	113.7 ± 1.1	26
quinoxaline[d]	$C_8H_6N_2$	HEYJOK08	$P2_12_12_1$	5/20	3.996	23.022	35.822	90.00	90.00	90.00	70.9 ± 0.3	28

[a]With the exception of benzene, all energetic data refer to 298.15 K, and the corresponding crystal structures were determined at room temperature. [b]Cambridge crystallographic database reference code.[20] [c]Data at 270 K. [d]Enthalpies of sublimation determined in this work by Calvet-drop microcalorimetry (see the Supporting Information for details).

J. Phys. Chem. A 2015, 119, 3023−3034
DOI: 10.1021/jp512349r

methods, the APC of hydrogen atoms located in the equivalent position were averaged.[9]

Polarizable Model. The polarizable model selected in this work (model B) was introduced in order to allow a readjustment of the APC in the original OPLS-AA parametrization to the local electrostatic environment generated by the neighbor molecules in the crystal structure. In the present case, the classical Drude oscillator model (also referred as Shell or Charge-on-Spring method) was considered.[40,41,50] By this method, a floating charge (Drude) connected by an harmonic spring to the atom core is used to create an induced dipole moment, $\vec{\mu}^{\text{ind}}$, in an atom, when submitted to an electric field, $\vec{E}$, so that

$$\vec{\mu}^{\text{ind}} = \alpha \cdot \vec{E} \tag{3}$$

where α is the atom polarizability.

In this work, the harmonic spring constant, k, was kept equal to 2092 kJ mol^{-1} for all atoms, while the Drude charge, q_{drud}, was computed from[50]

$$q_{\text{drud}} = -\sqrt{4\pi\varepsilon_o \alpha k} \tag{4}$$

The recommended atomic polarizabilities by Bica and co-workers[51] (α = 1.367 Å^3 for carbon, α = 0.641 Å^3 for oxygen, and α = 1.123 Å^3 for nitrogen) were used in eq 4.

The charge of the atom core, q_{core}, was calculated from

$$q_{\text{core}} = q_{\text{opls}} - q_{\text{drud}} \tag{5}$$

so that the sum of q_{drud} with q_{core} corresponds to the atomic point charge in the OPLS-AA force field, q_{opls}. The Drude particles were only assigned to nonhydrogen atoms and the interaction between the core and floating charges ignored. Here it should also be mentioned that eq 4 refers to all Drude charges being negative and their counterparts being positive.

In the present work, the adiabatic method was followed to allow a dynamical description of all particles.[52] In this sense, a fraction of the atomic mass, 0.3 amu, was transferred from the atom core to the Drude particle. The combination of this unusually high mass in the floating charge (that is normally set to 0.1 amu),[50] along with the use of a large and fixed spring constant (2092 kJ mol^{-1}), were selected so that simulations could be performed with a time step between 0.5 and 1 fs. To ensure that the kinetic energy of the Drude particles is negligible in relation to the total kinetic energy, the temperature of the moving charges was set to T < 1.0 K.[50,53] A Nosé–Hoover thermostat and barostat were used in the simulations, with relaxation time constants of 0.01–0.005 ps and 0.5–0.1 ps, respectively. The ranges given for the time step and relaxation constants are related to the need to adapt the simulation conditions for obtaining stable runs. As in the case of the simulations performed for the other models, an equilibration period of 0.3 ns and a production stage of 0.6 ns were performed. Further details about the use of the Drude model with the adiabatic method can be found elsewhere.[41,50,52]

One of the problems of using a floating charge model is related with the occurrence of a polarizable catastrophe. This is caused by a large displacement of the Drude particle in relation to the atom core, creating a huge dipole moment, which culminates in an abnormal increase of the system energy. In part, can avoid this effect by ensuring that the floating charges have a low temperature, but, due to the close proximity of bonded atoms, the polarizable catastrophe can still occur. To solve this problem, Thole proposed the use of screening functions to decrease the dipole–dipole interaction at close distances.[54] The software used in this work, DLPOLY package, does not have this option available for the simulations, thus, an alternative approach was followed. Following the exclusion rules assumed in the OPLS-AA force field, all core–core, core–Drude, and Drude–Drude, intramolecular interactions between atoms separated by one or two bonds were ignored and those between atoms separated by three bonds were scaled by 0.5.

RESULTS AND DISCUSSION

Experimental Data. As stated above, although experimental, structural, and energetic data can be found in the literature for organic compounds, only a few enthalpies of sublimation can be safely assigned to a definite crystal structure at the same temperature.[9] Thus, the first step was the collection of reliable experimental data available in the literature to establish a benchmark database (Table 1). In order to increase the variability of organic compounds and the number of structures containing more than one molecule in the asymmetric unit (Z′) in the list, the enthalpies of sublimation of vanillin (Z′/Z = 4/8), maleic acid (Z′/Z = 1/4), methylparaben (Z′/Z = 3/12), and quinoxaline (Z′/Z = 5/20) were also determined in this work (please see the Supporting Information for details). In the case of benzene, phenol, and benzoic acid, the available enthalpies of sublimation could not be directly ascribed to a particular crystal structure. Thus, in these cases, a critical analysis of the data in the literature was performed.

Benzene. At least 5 polymorphs for this compound have been reported and, at 1 bar of pressure, the known stable phase belongs to space group *Pbca*.[81] Thus, a match between the temperature of determination of the single crystal results for this space group, and the reported energetic data was executed. Jackowski[66] and Ha et al.[82] determined the enthalpy of sublimation of benzene from a series of vapor pressure results obtained in the temperature range from 220 to 278 K. Since Cox and co-workers[68] reported the crystal structure for benzene at ambient pressure and 270 K, the vapor pressures mentioned above were used to calculate the enthalpy of sublimation of this compound also at 270 K (details of this calculation are given as Supporting Information).

Phenol. In the case of phenol, at ambient pressure, two crystal structures were reported: one belonging to space group $P2_122_1$ and the other to $P_{11}2_1$.[80] However, the comparison of the two structures reveals that both are equivalent (please see comparison of the powder patterns simulated for both structures in Supporting Information). Thus, in this case, the enthalpy of sublimation at 298.15 K was computed from the enthalpies of formation of phenol recommended by Pedley[55] and the structure obtained by Gillier-Pandraud et al.[56] at room temperature ascribed to this value.

Benzoic Acid. The crystal structure of this compound was reported in the literature 12 times and, in all cases, the same phase was obtained. This suggests that benzoic acid is resilient to produce polymorphs and, as a consequence, any energetic data in the literature must correspond to the known structure. Thus, the enthalpy of sublimation recommended by Sabbah et al.[60] at 298.15 K and the crystal structure found by Feld et al.[59] at ambient temperature, were selected in this work.

All the remaining experimental results in Table 1 were taken from publications where the enthalpy of sublimation at 298.15 K was (or could be) determined for a specific crystal structure.

DOI: 10.1021/jp512349r
J. Phys. Chem. A 2015, 119, 3023–3034

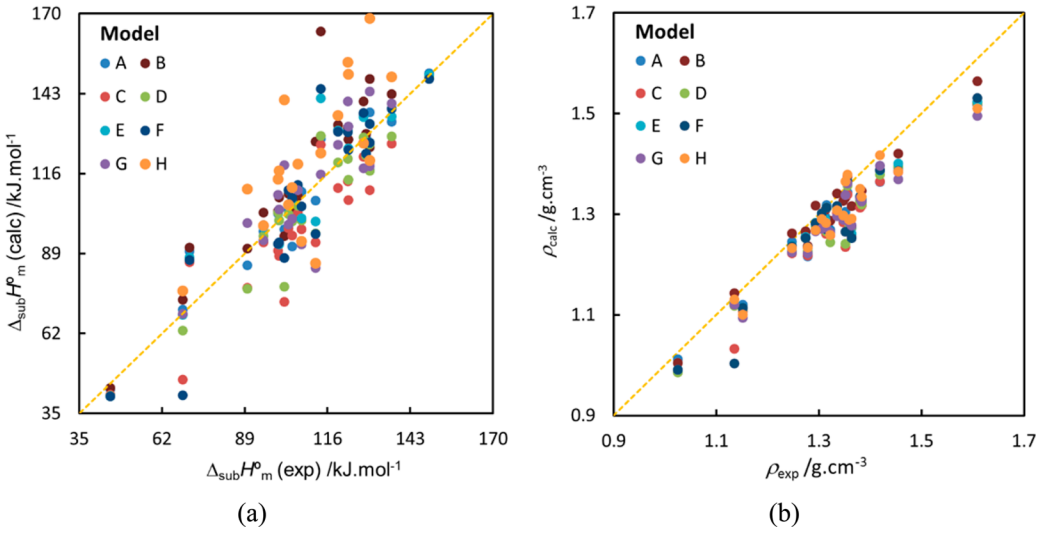

Figure 2. Comparison of experimental and computed (a) enthalpies of sublimation and (b) solid densities.

Computation Results. The molecular dynamics simulation results, obtained for each crystal structure in Table 1 and eight models explored in this work, are given as Supporting Information. Because no intermolecular hydrogen bonds are present in the crystal structures of benzene, quinoxaline, and heptacyclene, models G and H were not used in these cases.

When the APCs computed by models G and H are compared with those found with models C and E is observed, in some cases the charge of the same atom can vary almost 50% (please see APCs given as Supporting Information). Although, as discussed below, this variation does not significantly affect the quality of the computed structural parameters, thus suggesting that the molecular electrostatic environment is accurately captured, this difference has a strong impact in the computation of $U^{o}_{conf,m}$ (g). If, as previously proposed,[9] the computation of $\Delta_{sub}H^{o}_{m}$ by models H and G use $U^{o}_{conf,m}$(g) values obtained with APC computed for isolated molecules in the gaseous phase (in this case, models C and E) then huge differences between experimental and computed enthalpies of sublimation are observed. Thus, for each model investigated in this work, the same APCs were used in the calculation of $U^{o}_{conf,m}$ (cr) and $U^{o}_{conf,m}$ (g).

In general, all performed simulations led to successful runs. However, five exceptions were observed. The first three cases were found for the models based on the calculation of APC for isolated molecules in the gaseous phases using DFT functionals (model E and F). These models have led to the deformation of the simulation box of benzoic acid and salicylamide (only in the case of model E), resulting in the stabilization of the structure in a different crystallographic phase. The remaining cases were observed for the computation of crystal structures of *E*-heptacyclene and 2,2,5,7,8-pentamethylchroman-6-ol using the polarizable force field (model B), where despite all the efforts, it was found impossible to run stable simulations.

The origin of the problematic electronic charge distribution obtained when the DFT functionals were used in the computation of the APC of benzoic acid and salicylamide is difficult to identify. In fact, as can be observed in the atomic point charges given as Supporting Information, differences of 0.1 a.c.u can be found if the charges computed for the same atom by models C−F are compared (please remember that these are based in calculation with single molecules in the gaseous phase). This is the case, for example, of paracetamol, where despite the huge dissimilarity between APC found by the different methods, the theoretical predictions (both structural and energetic) agree fairly well with the experiment (see charges in table S23 and simulation results in Tables S46 and S47 of the Supporting Information). Thus, different sets of APC can lead to similar electrostatic environments, making the identification of APC calculation problems difficult to address without performing a simulation run.

With regard to the simulation of salicylamide, in general, all methods show equilibration problems. For this reason, all reported data for salicylamide were obtained after simulation runs with equilibration and production stages of 0.6 and 5 ns, respectively. It was also observed that, except in the case of models A, G, and H, the simulation leads to a triclinic unit cell instead of a monoclinic, with angles α and γ slightly different from 90 deg.

In order to evaluate the performance of the different models to compute energetic and unit cell parameters of each crystal structure indicated in Table 1, several types of analyses were performed. In Figure 2, the experimental densities and enthalpies of sublimation were plotted against the computed values. Figure 2a reveals that models B and H tend to overestimate the experimental enthalpies of sublimation, while model C shows the opposite trend. For the remaining models, no clear tendency to under/overestimate is observed. With regard to the density results (Figure 2b), in general, all methods lead to lower density values than in the experiment.

The maximum and the absolute average of the errors of the computed unit cell edges, angles, and density relative to the experimental data are given in Figure 3. If the average is considered, all the methods are approximately equivalent, with models C and F with an overall average deviation slightly higher than the remaining ones. Even so, in these two cases, the average deviation is lower than 4.1%, a result that is close to the typical deviations observed between MD simulation results and experimental values.[9,10,83,84] When the maximum deviations are considered (Figure 3), a different picture emerges: (i) models A, B, C, D, and E are, more and less, equivalent; (ii) model F exhibits the bigger deviations for all three properties evaluated; and (iii) models G and H led, overall, to a lower maximum deviation. Thus, MD simulations performed using atomic point

DOI: 10.1021/jp512349r
J. Phys. Chem. A 2015, 119, 3023−3034

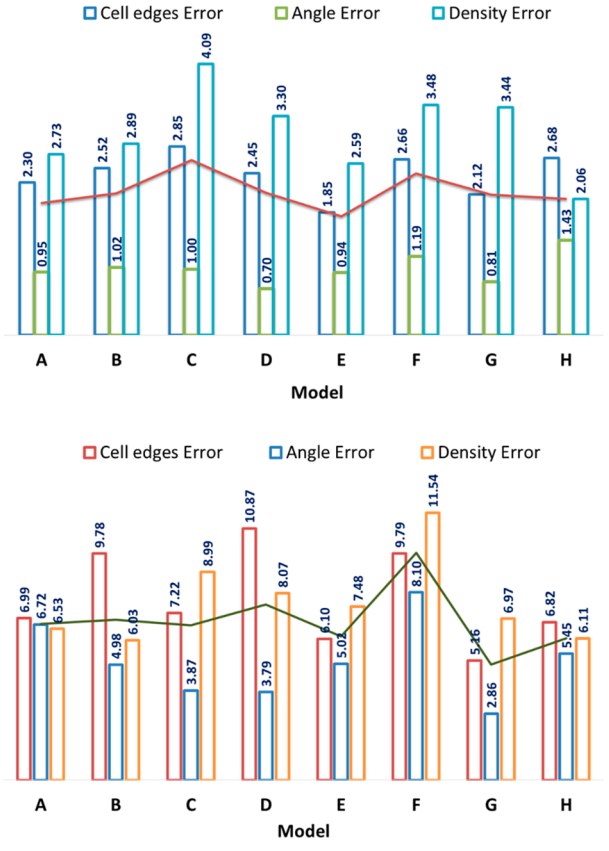

Figure 3. Absolute average (top) and maximum (bottom) percentage errors of the unit cell parameters, found from the molecular dynamic simulations with the different theoretical models explored in this work. The solid lines represent the average of the cell edges, angle, and density errors found for each model.

charges computed, taking into account the neighborhood of each molecule in the asymmetric unit, lead to lower maximum deviations to the experimental results, suggesting that the electrostatic environments in the crystal structure is properly captured by models G and H. Furthermore, because only molecules connected by hydrogen bonds are considered in these models, the target molecules are still sufficient, exposed to obtain good quality charges by the ChelpG methodology, avoiding problems normally associated with the existence of buried atoms.[49] It is also interesting to note that, although polarization seems to be important to the calculation of the APC, the use of the polarizable model B did not significantly improve the results, when compared with those found with the original OPLS-AA force field (model A).

From the energetic point of view, Figure 4, large deviations are observed between computed and experimental enthalpies of sublimation. The lower average deviations are observed for the original OPLS-AA force field, model A (5.5 kJ mol^{-1}), followed by models D (6.7 kJ mol^{-1}) and E (6.9 kJ mol^{-1}), both based on APC computed for a single molecule in the gaseous phase at MP2/aug-cc-pVDZ and B3PW91/6-311+G(d,p) levels of theory, respectively. Furthermore, these three models also lead to the lower maximum deviations when compared with the experimental values.

The large deviations discussed above can be explained, at least in part, by the necessity to determine the molecular internal energy to compute the enthalpies of sublimation (please see eq 2). In fact, because a flexible model was used in

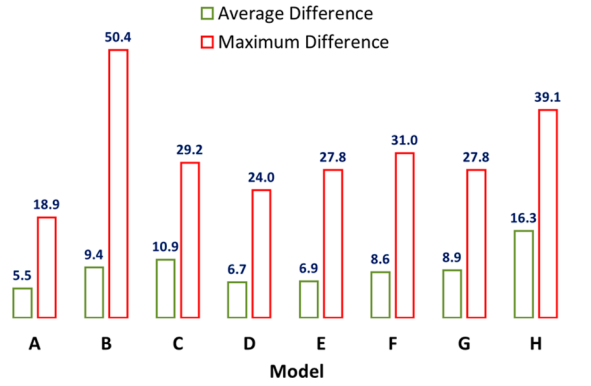

Figure 4. Absolute average and maximum differences between computed and experimental enthalpies of sublimation. Data in kJ mol^{-1}.

all simulations, the molecular internal contribution to the configurational energy of the solid has to be evaluated. However, as mentioned in Methods, due to the small size of the system, a poor statistic is obtained during the computation of $U^{o}_{conf,\,m}$ (g). This is reflected, in a large dispersion of the computed internal energies that can represent, in some cases, a difference of more than 20 kJ mol^{-1} between the maximum and minimum values of $U^{o}_{conf,\,m}$ (g). Even so, for example, the average difference of 5.7 kJ mol^{-1} observed for model A is within typical deviations observed between experimental and computed enthalpies of sublimation, estimated using rigid molecules, force fields specifically designed for the simulation of solids, and a test set significantly smaller than that considered in this work.[5]

As important as the accuracy in the prediction of enthalpies of sublimations is the ability to determine the relative order of stability of different phases. In order to evaluate this feature, Figure 5 shows the comparison of computed enthalpies of transition, $\Delta_{trs}H$, for the different systems given in Table 1. These results were obtained from

$$\Delta_{trs}H(\mathrm{A} \rightarrow \mathrm{B}) = \Delta_{sub}H^{o}_{m}(\mathrm{A}) - \Delta_{sub}H^{o}_{m}(\mathrm{B}) \qquad (6)$$

where $\Delta_{sub}H^{o}_{m}(\mathrm{A})$ and $\Delta_{sub}H^{o}_{m}(\mathrm{B})$ are the enthalpies of sublimation of phases A and B. The choice of using the enthalpies of sublimation to evaluate $\Delta_{trs}H$ is related with the fact that, different phases can imply different molecular conformations that, in turn, can lead to significantly different internal contributions to the configurational energy of the crystal. $\Delta_{trs}H$ represents the enthalpic difference between lattice energies and should not reflect differences in the internal energy of the molecules. This is especially evident in the case of the determination of the transformation energy between the two isomers of heptacyclene in the solid state. Furthermore, because the enthalpies of sublimation used to compute $\Delta_{trs}H$ refer to a similar compound, it is expected that $\Delta_{sub}H^{o}_{m}$ obtained for the phases under consideration will be affected by similar errors in the evaluation of $U^{o}_{conf,\,m}$ (g). Thus, an elimination of systematic errors is expected to occur when eq 6 is used.

The analysis of Figure 5 reveals that, in majority of cases, an inverse order of stability is predicted outside the combined uncertainties of the $\Delta_{trs}H$ values. The exception is found for method G that, considering the errors of the determinations, forecast the order of stability of the phases for all systems. Even so, this method predicts an enthalpic difference significantly

DOI: 10.1021/jp512349r
J. Phys. Chem. A 2015, 119, 3023−3034

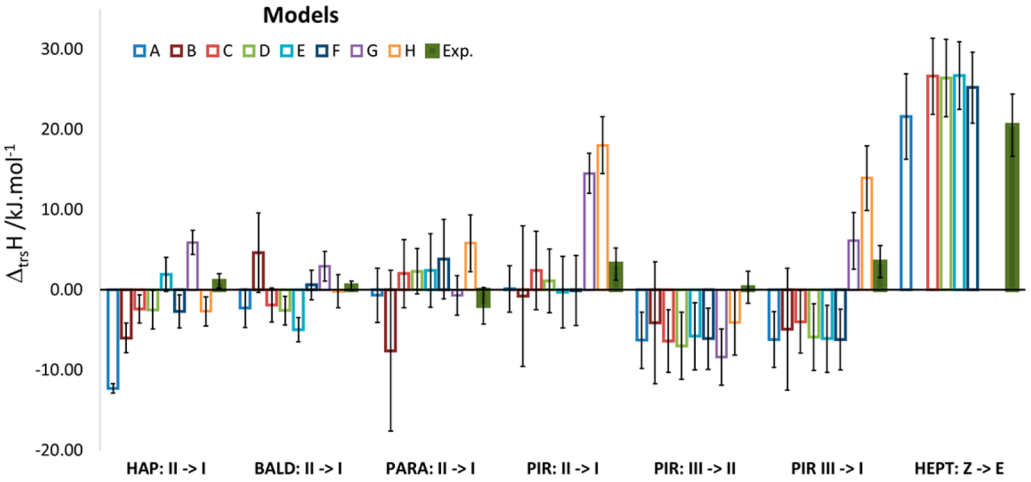

Figure 5. Computed and experimental (Exp.) enthalpies of phase transition, $\Delta_{trs}H$, between the polymorphs of 4′-hydroxyacetophenone (HAP), 4-hydroxybenzaldehyde (BALD), paracetamol (PARA) and piracetam (PIR), and heptacyclene (HEPT) isomers in the solid state.

bigger between the polymorphs of 4′-hydroxyacetophenone and piracetam than that observed experimentally. Another interesting conclusion taken from Figure 5 is that the inclusion of polarization to the original OPLS-AA force field (model B) resulted in the improvement of the calculation of $\Delta_{trs}H$. Actually, if the result obtained for the transition enthalpy of 4′-hydroxyacetophenone is ignored (that even so, improved significantly with the inclusion of polarizability), the use of model B almost leads to the agreement between theoretical and experimental $\Delta_{trs}H$ values, within the combined errors of the determinations.

Finally, in order to evaluate the ability of the different methods to predict the structure and energetic data of different crystal phases, in Figure 6, the plot of the sum of the module of the cell dimensions, angle and density errors, $\Sigma|\%_{error,\ struc}|$, against the corresponding module of the difference between computed and experimental enthalpies of sublimation is represented. The two dash lines represent the limit for an acceptable deviation between experimental and theoretical values. The vertical line has been drawn considering that, in order to obtain a good agreement between $\Delta_{sub}H^{o}_{m}$ data, a difference between values should be inferior to 6.5 kJ mol^{-1}. This limit was found as the sum of the average errors associated with the theoretical evaluation of $\Delta_{sub}H^{o}_{m}$ (~4.0 kJ mol^{-1}; see results in the Supporting Information), with the average errors of the experimental enthalpies of sublimation (~2.5 kJ mol^{-1}). The horizontal line, corresponds to a sum of errors of 7.5% and assumes that each of the three structural properties evaluated can exhibit a deviation as big as ~2.5%.

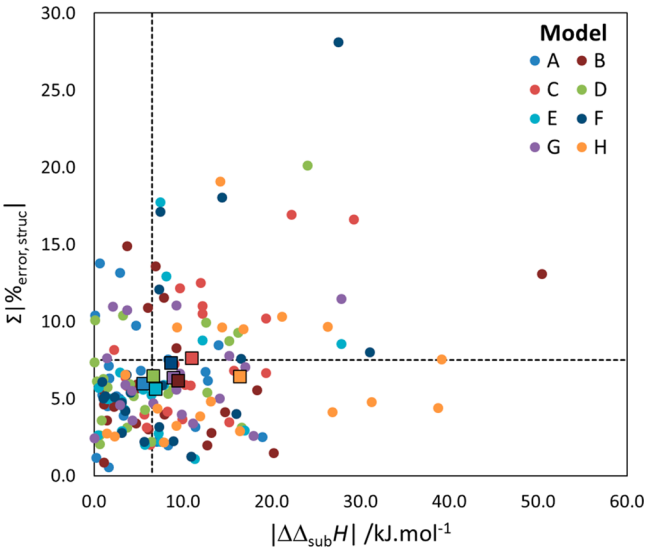

Figure 6. Representation of the sum of the module of cell edges, angle, and density errors, ($\Sigma|\%_{error,\ struc}|$) relative to the corresponding module of the difference between computed and experimental enthalpies of sublimation, $\Delta\Delta_{sub}H$, for all possible combinations of molecules and models investigated in this work. The dash lines delineate the maximum acceptable deviation between the experimental and theoretical data (see text for details). The squared dots represent the averages observed for each model.

Figure 6 reveals that, overall, only ~33% of the computed results are in good agreement with the experimental data. Furthermore, as highlighted above, a better agreement between computed and experimental data is found for the structural features than for energetics: approximately 71% of the calculated unit cell parameters agree with the experiment, against only 47% of the calculated enthalpies of sublimation.

When the data for each method is evaluated individually, it is found that, with the exception of model C, on average, all the remaining models give deviations below the threshold defined for the structural parameters, but, only methods A (original OPLS-AA force field) and D (that uses MP2/aug-cc-pVDZ APC computed for a single molecule) show average deviations to the experimental results close or within the energetic limit (see squared dots in Figure 6). In fact, the latter methods reproduced the unit cell parameters for 17 out of the 23 crystal structures evaluated. In terms of enthalpy of sublimation, model A accurately reproduced the experimental values 15 times and model D, 14. On the other hand, model D shows the best simultaneous agreement between structural and energetic data (12 structures), followed by models A and F (with 11 structures; model F is based in B3LYP/6-311+G(d,p) APC found for single molecules). The lower performance to reproduce experimental data was found for model H (that uses B3PW91/6-311+G(d,p) charges computed for a cluster of molecules), with only three compounds agreeing simultaneously in terms of structure and enthalpy of sublimation. Finally, no relation between the number of molecules in the

DOI: 10.1021/jp512349r
J. Phys. Chem. A 2015, 119, 3023−3034

asymmetric unit of the crystal structure and the quality of the computed results by the different methods was observed.

CONCLUSIONS

One of the main objectives of this work was the evaluation of OPLS-AA force field ability to study organic compounds in the solid state. Furthermore, it was intended to investigate if the original parametrization could be improved for the examination of the properties of these materials. The results here gathered suggest that the force field without any modification can be a good starting point for the study of the main features of crystal structures, but an assessment is always recommended. The replacement of the original OPLS-AA atomic point charges by values derived for the crystal environment at the MP2/cc-pVDZ level of theory (model G) leads to lower maximum deviations when the structural parameters are evaluated. This suggests that the used of crystal-derived APC, using the methodology described in this work, is able to capture the main features of the electrostatic environment of crystal structures.

The importance of a good description of the electrostatic environment in the study of crystal structures is also evidenced in the use of the polarizable model B. Although, in general, this model did not lead to an improvement of the computed results, it captures the enthalpic difference between polymorphs more accurately. This suggests that, for example, when hydrogen bonds are present in the crystal structure the averaged implicit electronic polarization that results from the fitting of the OPLS-AA parameters to the experimental properties of organic liquids[18] is not sufficient to properly distinguish crystal structures from an energetic point of view.

In general, the analysis of the obtained results propose that, depending on the properties of the solid material to be investigated, improvements to the description of the electrostatic interaction between the molecules can be introduced: (1) *Study the solution dynamics*: these studies are often used to investigate the formation of solids from solution. In this sense, due to the small energetic difference observed between polymorphs that can be formed, a good description of the energetic difference of the phases is desirable. For this reason, methods B (polarizable OPLS-AA force field) and G (that relies on the use of MP2/cc-pVDZ APC computed for molecules taking into consideration their local environment) are recommended (Figure 5). (2) *Study of structural features*: because all investigated methods exhibit similar average deviations to the experimental single crystal data, the recommendation lies in the use of method G, since it exhibits the lower maximum deviations to the experimental results (Figure 3). (3) *Evaluation of lattice energies*: for this type of study, the use of model A (the original OPLS-AA force field) is recommended since it reproduced the experimental enthalpies of sublimation with the lower average and maximum deviations (Figure 4). (4) *Structural and energetic studies*: as exhibited in Figure 6, overall, the use of models A and D (that uses MP2/aug-cc-pVDZ APC found for a single molecule) seem to be the best approach to simultaneously predict the unit cell parameters and enthalpy of sublimation of organic compounds.

Relative to the quantum chemical calculations, the obtained results suggest that the use of density functional theory methods to compute APC can lead to unpredictable results, as observed for the case of benzoic acid. On the other hand, the MP2 method, especially with basis sets containing polarization and diffuse functions, seem to be an appropriate selection for the evaluation of APC.

ASSOCIATED CONTENT

Supporting Information

Part I: full refs 3, 17, and 32. Part II: details of enthalpy of sublimation determination of vanillin, maleic acid, methylparaben, and quinoxaline, and the redetermination of the enthalpy of sublimation of benzene. Part III: details of the molecular dynamic simulations, the schematic view of the OPLS-AA nomenclature used to create the force field file also available as Supporting Information and, finally, the APC obtained for each model. Part IV: simulation results for the different methods and structures investigated in this work. This material is available free of charge via the Internet at http://pubs.acs.org.

AUTHOR INFORMATION

Corresponding Author

*E-mail: cebernardes@ciencias.ulisboa.pt.

Notes

The authors declare no competing financial interest.

ACKNOWLEDGMENTS

This work was supported by Fundação para a Ciência e a Tecnologia (FCT), Portugal (Projects PTDC/QUI-QUI/116847/2010, PEst-OE/QUI/UI0100/2013, and PEst-OE/QUI/UI0612/2013). A. Joseph and C. Bernardes also gratefully acknowledge a Ph.D. and a post doctoral grant from FCT (SFRH/BD/90386/2012 and SFRH/BPD/101505/2014), respectively. We thank Professors Manuel Minas da Piedade, José Nuno Canongia Lopes, and Prof. Hermínio Diogo for useful discussions that helped improve this work.

REFERENCES

(1) Price, S. L. Predicting Crystal Structures of Organic Compounds. *Chem. Soc. Rev.* **2014**, *43*, 2098−2111.

(2) Bhardwaj, R. M.; Price, L. S.; Price, S. L.; Reutzel-Edens, S. M.; Miller, G. J.; Oswald, I. D. H.; Johnston, B. F.; Florence, A. J. Exploring the Experimental and Computed Crystal Energy Landscape of Olanzapine. *Cryst. Growth Des.* **2013**, *13*, 1602−1617.

(3) Bardwell, D. A.; Adjiman, C. S.; Arnautova, Y. A.; Bartashevich, E.; Boerrigter, S. X. M.; Braun, D. E.; Cruz-Cabeza, A. J.; Day, G. M.; Della Valle, R. G.; Desiraju, G. R.; et al. Towards Crystal Structure Prediction of Complex Organic Compounds: A Report on the Fifth Blind Test. *Acta Crystallogr., Sect. B* **2011**, *67*, 535−551.

(4) Davey, R. J.; Schroeder, S. L. M.; ter Horst, J. H. Nucleation of Organic Crystals- A Molecular Prspective. *Angew. Chem., Int. Ed.* **2013**, *52*, 2166−2179.

(5) Williams, D. E. Improved Intermolecular Force Field for Molecules Containing H, C, N, and O Atoms, with Application to Nucleoside and Peptide Crystals. *J. Comput. Chem.* **2001**, *22*, 1154−1166.

(6) Cox, S. R.; Hsu, L. Y.; Williams, D. E. Nonbonded Potential Function Models for Crystalline Oxohydrocarbons. *Acta Crystallogr., Sect. A* **1981**, *37*, 293−301.

(7) Williams, D. E.; Cox, S. R. Nonbonded Potentials for Azahydrocarbons: The Importance of the Coulombic Interaction. *Acta Crystallogr., Sect. B* **1984**, *40*, 404−417.

(8) Day, G. M.; Chisholm, J.; Shan, N.; Motherwell, W. D. S.; Jones, W. Assessment of Lattice Energy Minimization for the Prediction of Molecular Organic Crystal Structures. *Cryst. Growth Des.* **2004**, *4*, 1327−1340.

(9) Bernardes, C. E. S.; Minas da Piedade, M. E.; Canongia Lopes, J. N. Polymorphism in 4′-Hydroxyacetophenone: A Molecular Dynamics Simulation Study. *J. Phys. Chem. B* **2012**, *116*, 5179−5184.

(10) Bernardes, C. E. S.; Lopes, J. N. C.; Minas da Piedade, M. E. All-Atom Force Field for Molecular Dynamics Simulations on Organo-transition Metal Solids and Liquids. Application to $M(CO)_n$ (M = Cr,

DOI: 10.1021/jp512349r
J. Phys. Chem. A 2015, 119, 3023−3034

Fe, Ni, Mo, Ru, or W) Compounds. *J. Phys. Chem. A* **2013**, *117*, 11107−11113.
(11) Simões, R. G.; Bernardes, C. E. S.; Minas da Piedade, M. E. Polymorphism in 4-Hydroxybenzaldehyde: A Crystal Packing and Thermodynamic Study. *Cryst. Growth Des.* **2013**, *13*, 2803−2814.
(12) Dupradeau, F. Y.; Pigache, A.; Zaffran, T.; Savineau, C.; Lelong, R.; Grivel, N.; Lelong, D.; Rosanski, W.; Cieplak, P. The R.ED. Tools: Advances in RESP and ESP Charge Derivation and Force Field Library Building. *Phys. Chem. Chem. Phys.* **2010**, *12*, 7821−7839.
(13) Gavezzotti, A. Non-conventional Bonding Between Organic Molecules. The 'Halogen Bond' in Crystalline Systems. *Mol. Phys.* **2008**, *106*, 1473−1485.
(14) Leslie, M. DL_MULTI: A Molecular Dynamics Program to Use Distributed Multipole Electrostatic Models to Simulate the Dynamics of Organic Crystals. *Mol. Phys.* **2008**, *106*, 1567−1578.
(15) Cornell, W. D.; Cieplak, P.; Bayly, C. I.; Gould, I. R.; Merz, K. M.; Ferguson, D. M.; Spellmeyer, D. C.; Fox, T.; Caldwell, J. W.; Kollman, P. A. A 2nd Generation Force-Field for the Simulation of Proteins, Nucleic-Acids, and Organic-Molecules. *J. Am. Chem. Soc.* **1995**, *117*, 5179−5197.
(16) Wang, J. M.; Kollman, P. A. Automatic Parameterization of Force Field by Systematic Search and Genetic Algorithms. *J. Comput. Chem.* **2001**, *22*, 1219−1228.
(17) MacKerell, A. D.; Bashford, D.; Bellott, M.; Dunbrack, R. L.; Evanseck, J. D.; Field, M. J.; Fischer, S.; Gao, J.; Guo, H.; Ha, S.; et al. All-Atom Empirical Potential for Molecular Modeling and Dynamics Studies of Proteins. *J. Phys. Chem. B* **1998**, *102*, 3586−3616.
(18) Jorgensen, W. L.; Maxwell, D. S.; Tirado-Rives, J. Development and Testing of the OPLS All-Atom Force Field on Conformational Energetics and Properties of Organic Liquids. *J. Am. Chem. Soc.* **1996**, *118*, 11225−11236.
(19) Kaminski, G.; Jorgensen, W. L. Performance of the AMBER94, MMFF94, and OPLS-AA Force Fields for Modeling Organic Liquids. *J. Phys. Chem.* **1996**, *100*, 18010−18013.
(20) Allen, F. H. Cambridge Structural Database. *Acta Crystallogr.* **2002**, *B58*, 380−388.
(21) Breneman, C. M.; Wiberg, K. B. Determining Atom-Centered Monopoles from Molecular Electrostatic Potentials: The Need for High Sampling Density in Formamide Conformational-Analysis. *J. Comput. Chem.* **1990**, *11*, 361−373.
(22) Mackerell, A. D.; Karplus, M. Importance of Attractive van der Waals Contribution in Empirical Energy Function Models for the Heat of Vaporization of Polar Liquids. *J. Phys. Chem.* **1991**, *95*, 10559−10560.
(23) Laugier, J.; Bochu, B. *CELREF*, Version 3, 1997.
(24) Bernardes, C. E. S.; Minas da Piedade, M. E. Energetics of the O-H Bond and of Intramolecular Hydrogen Bonding in $HOC_6H_4C(O)Y$ (Y = H, CH_3, $CH_2CH{=}CH_2$, $C{\equiv}CH$, CH_2F, NH_2, $NHCH_3$, NO_2, OH, OCH_3, OCN, CN, F, Cl, SH, and SCH_3) Compounds. *J. Phys. Chem. A* **2008**, *112*, 10029−10039.
(25) Velavan, R.; Sureshkumar, P.; Sivakumar, K.; Natarajan, S. Vanillin-I. *Acta Crystallogr., Sect. C* **1995**, *51*, 1131−1133.
(26) James, M. N. G.; Williams, G. J. Refinement of Crystal-Structure of Maleic Acid. *Acta Crystallogr., Sect. B* **1974**, *30*, 1249−1257.
(27) Xianti, L.; Huaxue, J. *Chin. J. Struct. Chem.* **1983**, *2*, 213.
(28) Sathishkumar, R.; Mahapatra, S.; Thakur, T. S.; Desiraju, G. R. Dimorphism and Structural Modulation in Quinoxaline. *Curr. Sci.* **2010**, *99*, 1807−1811.
(29) Kiyobayashi, T.; Minas da Piedade, M. E. The Standard Molar Enthalpy of Sublimation of η^5-Bis-pentamethylcyclopentadienyl Iron Measured with an Electrically Calibrated Vacuum-Drop Sublimation Microcalorimetric Apparatus. *J. Chem. Thermodyn.* **2001**, *33*, 11−21.
(30) Bernardes, C. E. S.; Santos, L. M. N. B. F.; Minas da Piedade, M. E. A New Calorimetric System to Measure Heat Capacities of Solids by the Drop Method. *Meas. Sci. Technol.* **2006**, *17*, 1405−1408.
(31) Joseph, A.; Bernardes, C. E. S.; da Piedade, M. E. M. Heat Capacity and Thermodynamics of Solid and Liquid Pyridine-3-carboxylic Acid (Nicotinic Acid) Over the Temperature Range 296 to 531 K. *J. Chem. Thermodyn.* **2012**, *55*, 23−28.
(32) Frisch, M. J.; Trucks, G. W.; Schlegel, H. B.; Scuseria, G. E.; Robb, M. A.; Cheeseman, J. R.; Montgomery, J. A., Jr.; Vreven, T.; Kudin, K. N.; Burant, J. C.; et al. *Gaussian 03*, revision C.02. Gaussian, Inc.: Wallingford, CT, 2004.
(33) Becke, A. D. Density-Functional Thermochemistry. III. The Role of Exact Exchange. *J. Chem. Phys.* **1993**, *98*, 5648−5652.
(34) Lee, C.; Yang, W.; Parr, R. G. Development of the Colle-Salvetti Correlation-Energy Formula into a Functional of the Electron-Density. *Phys. Rev. B* **1988**, *37*, 785−789.
(35) Frisch, M. J.; Pople, J. A.; Binkley, J. S. Self-Consistent Molecular-Orbital Methods 0.25. Supplementary Functions for Gaussian-Basis Sets. *J. Chem. Phys.* **1984**, *80*, 3265−3269.
(36) In *NIST Standard Reference Database 101 (Release 16a)*; National Institute of Standards and Technology: Gaithersburg, MD, 2013.
(37) Smith, W.; Forester, T. R. The DL_POLY Package of Molecular Simulation Routines (v.2.2); The Council for The Central Laboratory of Research Councils, Daresbury Laboratory: Warrington, Cheshire, U.K., 2006.
(38) Bernardes, C. E. S. *DLPGEN*, V1.0, Generator of Input Files for the DLPOLY Program; available from the authors, 2014.
(39) Mohr, P. J.; Taylor, B. N.; Newell, D. B. CODATA Recommended Values of the Fundamental Physical Constants: 2010. *Rev. Mod. Phys.* **2012**, *84*, 1527−1605.
(40) Lamoureux, G.; MacKerell, A. D.; Roux, B. A simple polarizable model of water based on classical Drude oscillators. *J. Chem. Phys.* **2003**, *119*, 5185−5197.
(41) Anisimov, V. M.; Lamoureux, G.; Vorobyov, I. V.; Huang, N.; Roux, B.; MacKerell, A. D. Determination of Electrostatic Parameters for a Polarizable Force Field Based on the Classical Drude Oscillator. *J. Chem. Theory Comput.* **2005**, *1*, 153−168.
(42) Frisch, M. J.; Head-Gordon, M.; Pople, J. A. A Direct Mp2 Gradient-Method. *Chem. Phys. Lett.* **1990**, *166*, 275−280.
(43) Frisch, M. J.; Head-Gordon, M.; Pople, J. A. Semidirect Algorithms for the Mp2 Energy and Gradient. *Chem. Phys. Lett.* **1990**, *166*, 281−289.
(44) Head-Gordon, M.; Pople, J. A.; Frisch, M. J. Mp2 Energy Evaluation by Direct Methods. *Chem. Phys. Lett.* **1988**, *153*, 503−506.
(45) Head-Gordon, M.; Head-Gordon, T. Analytic Mp2 Frequencies without 5th-Order Storage: Theory and Application to Bifurcated Hydrogen-Bonds in the Water Hexamer. *Chem. Phys. Lett.* **1994**, *220*, 122−128.
(46) Woon, D. E.; Dunning, T. H. Gaussian-Basis Sets for Use in Correlated Molecular Calculations 0.3. The Atoms Aluminum through Argon. *J. Chem. Phys.* **1993**, *98*, 1358−1371.
(47) Perdew, J. P.; Wang, Y. Accurate and Simple Analytic Representation of the Electron-gas Correlation Energy. *Phys. Rev. B* **1992**, *45*, 13244−13249.
(48) Mclean, A. D.; Chandler, G. S. Contracted Gaussian-Basis Sets for Molecular Calculations. I. Second Row Atoms, Z = 11−18. *J. Chem. Phys.* **1980**, *72*, 5639−5648.
(49) Bayly, C. I.; Cieplak, P.; Cornell, W. D.; Kollman, P. A. A Well-Behaved Electrostatic Potential Based Method Using Charge Restraints for Deriving Atomic Charges: The Resp Model. *J. Phys. Chem.* **1993**, *97*, 10269−10280.
(50) Schröder, C.; Steinhauser, O. Simulating Polarizable Molecular Ionic Liquids with Drude Oscillators. *J. Chem. Phys.* **2010**, *133*.
(51) Bica, K.; Deetlefs, M.; Schröder, C.; Seddon, K. R. Polarisabilities of Alkylimidazolium Ionic Liquids. *Phys. Chem. Chem. Phys.* **2013**, *15*, 2703−2711.
(52) Mitchell, P. J.; Fincham, D. Shell-Model Simulations by Adiabatic Dynamics. *J. Phys.: Condens. Matter* **1993**, *5*, 1031−1038.
(53) Sprik, M. Computer-Simulation of the Dynamics of Induced Polarization Fluctuations in Water. *J. Phys. Chem.* **1991**, *95*, 2283−2291.
(54) Thole, B. T. Molecular Polarizabilities Calculated with a Modified Dipole Interaction. *Chem. Phys.* **1981**, *59*, 341−350.

DOI: 10.1021/jp512349r
J. Phys. Chem. A 2015, 119, 3023−3034

(55) Pedley, J. B. *Thermochemical Data and Structures of Organic Compounds*; Thermodynamics Research Center: College Station, Texas, 1994.
(56) Gillier-Pandraud, H. Crystalline Structure of Phenol. *Bull. Soc. Chim. Fr.* **1967**, 1988.
(57) Iwasaki, F. Refinement of p-hydroxybenzaldehyde. *Acta Crystallogr., Sect. B* **1977**, *33*, 1646−1648.
(58) Jasinski, J. P.; Butcher, R. J.; Narayana, B.; Swamy, M. T.; Yathirajan, H. S. Redetermination of 4-hydroxybenzaldehyde. *Acta Crystallogr., Sect. E* **2008**, *64*, O187.
(59) Feld, R.; Lehmann, M. S.; Muir, K. W.; Speakman, J. C. The Crystal-Structure of Benzoic-Acid: A Redetermination with X-Rays at Room-Temperature: A Summary of Neutron-Diffraction Work at Temperatures down to 5k. *Z. Kristallogr.* **1981**, *157*, 215−231.
(60) Sabbah, R.; An, X. W.; Chickos, J. S.; Leitao, M. L. P.; Roux, M. V.; Torres, L. A. Reference Materials for Calorimetry and Differential Thermal Analysis. *Thermochim. Acta* **1999**, *331*, 93−204.
(61) Bernardes, C. E. S.; Piedade, M. F. M.; Minas da Piedade, M. E. Polymorphism in 4′-hydroxyacetophenone: Structure and Energetics. *Cryst. Growth Des.* **2008**, *8*, 2419−2430.
(62) Gupta, M. P.; Kumar, P. *Cryst. Struct. Commun.* **1975**, 365.
(63) Goncalves, E. M.; Bernardes, C. E. S.; Diogo, H. P.; Minas da Piedade, M. E. Energetics and Structure of Nicotinic Acid (Niacin). *J. Phys. Chem. B* **2010**, *114*, 5475−5485.
(64) Pertlik, F. Crystal-Structures and Hydrogen-Bonding Schemes in 4 Benzamide Derivatives (2-Hydroxy-Benzamide, 2-Hydroxy-Thiobenzamide, 2-Hydroxy-N,N-Dimethyl-Benzamide, and 2-Hydroxy-N,N-Dimethyl-Thiobenzamide). *Monatsh. Chem.* **1990**, *121*, 129−139.
(65) Hansen, L. K.; Perlovich, G. L.; Bauer-Brandl, A. 4-Hydroxybenzamide. *Acta Crystallogr., Sect. E* **2007**, *63*, O2362−U2731.
(66) Jackowski, A. W. Vapor-Pressures of Solid Benzene and of Solid Cyclohexane. *J. Chem. Thermodyn.* **1974**, *6*, 49−52.
(67) Ha, H.; Morrison, J. A.; Richards, E. L. Vapor-Pressures of Solid Benzene, Cyclohexane and Their Mixtures. *J. Chem. Soc., Faraday Trans.* **1976**, *72*, 1051−1057.
(68) Cox, E. G.; Cruickshank, D. W. J.; Smith, J. A. S. The Crystal Structure of Benzene at −3-Degrees-C. *Proc. R. Soc. London, Ser. A* **1958**, *247*, 1−21.
(69) Welberry, T. R. Crystal and Molecular Structure of Cis-Dimer of Acenaphthylene. *Acta Crystallogr., Sect. B* **1971**, *27*, 360−365.
(70) Santos, R. C.; Bernardes, C. E. S.; Diogo, H. P.; Piedade, M. F. M.; Canongia Lopes, J. N.; Minas da Piedade, M. E. Energetics of the Thermal Dimerization of Acenaphthylene to Heptacyclene. *J. Phys. Chem. A* **2006**, *110*, 2299−2307.
(71) Haisa, M.; Kashino, S.; Kawai, R.; Maeda, H. Monoclinic Form of p-hydroxyacetanilide. *Acta Crystallogr., Sect. B* **1976**, *32*, 1283−1285.
(72) Picciochi, R.; Diogo, H. P.; Minas da Piedade, M. E. Thermochemistry of Paracetamol. *J. Therm. Anal. Calorim.* **2010**, *100*, 391−401.
(73) Drebushchak, T. N.; Boldyreva, E. V. Variable Temperature (100−360 K) Single-Crystal X-ray Diffraction Study of the Orthorhombic Polymorph of Paracetamol (p-hydroxyacetanilide). *Z. Kristallogr.* **2004**, *219*, 506−512.
(74) Louer, D.; Louer, M.; Dzyabchenko, V. A.; Agafonov, V.; Ceolin, R. Structure of a Metastable Phase of Piracetam from X-Ray-Powder Diffraction Using Atom-Atom Potential Method. *Acta Crystallogr., Sect. B* **1995**, *51*, 182−187.
(75) Picciochi, R.; Diogo, H. P.; Minas da Piedade, M. E. Thermodynamic Characterization of Three Polymorphic Forms of Piracetam. *J. Pharm. Sci.* **2011**, *100*, 594−603.
(76) Admiraal, G.; Eikelenboom, J. C.; Vos, A. Structures of the Triclinic and Monoclinic Modifications of (2-Oxo-1-Pyrrolidinyl)-Acetamide. *Acta Crystallogr., Sect. B* **1982**, *38*, 2600−2605.
(77) Galdecki, Z.; Glowka, M. L. Crystal-Structure of Nootropic Agent, Piracetam-2-Oxopyrrolidin-1-Ylacetamide. *Polym. J. Chem.* **1983**, *57*, 1307−1312.
(78) Mukai, K.; Ohbayashi, S.; Nagaoka, S.; Ozawa, T.; Azuma, N. X-Ray Crystallographic Studies of Vitamin-E Derivatives - Relationship Between Antioxidant Activity and Molecular-Structure. *Bull. Chem. Soc. Jpn.* **1993**, *66*, 3808−3810.
(79) Bernardes, C. E. S.; Simões, R. G.; Diogo, H. P.; Minas da Piedade, M. E. Thermochemistry of 2,2,5,7,8-pentamethylchroman-6-ol (PMC) and 6-hydroxy-2,5,7,8-tetramethylchroman-2-carboxylic Acid (Trolox). *J. Chem. Thermodyn.* **2014**, *73*, 140−147.
(80) Burton, G. W.; Doba, T.; Gabe, E. J.; Hughes, L.; Lee, F. L.; Prasad, L.; Ingold, K. U. Autoxidation of Biological Molecules. 4. Maximizing the Antioxidant Activity of Phenols. *J. Am. Chem. Soc.* **1985**, *107*, 7053−7065.
(81) Raiteri, P.; Martonak, R.; Parrinello, M. Exploring Polymorphism: The Case of Benzene. *Angew. Chem., Int. Ed.* **2005**, *44*, 3769−3773.
(82) Ha, H.; Morrison, J. A.; Richards, E. L. Vapor-Pressures of Solid Benzene, Cyclohexane and Their Mixtures. *J. Chem. Soc., Faraday Trans. 1* **1976**, *72*, 1051−1057.
(83) Canongia Lopes, J. N.; Couto, P. C.; Minas da Piedade, M. E. An All-Atom Force Field for Metallocenes. *J. Phys. Chem. A* **2006**, *110*, 13850−13856.
(84) Lousada, C. M.; Pinto, S. S.; Canongia Lopes, J. N.; Piedade, M. F. M.; Diogo, H. P.; Minas da Piedade, M. E. Experimental and Molecular Dynamics Dimulation Study of the Sublimation and Vaporization Energetics of Iron Metalocenes. Crystal Structures of $Fe(\eta^5\text{-}C_5H_4CH_3)_2$ and $Fe[\eta^5\text{-}(C_5H_5)(\eta^5\text{-}C_5H_4CHO)]$. *J. Phys. Chem. A* **2008**, *112*, 2977−2987.

DOI: 10.1021/jp512349r
J. Phys. Chem. A 2015, 119, 3023−3034